

Stability Limit Extension of a Wet Ethanol-fueled SI Engine using a Microwave-assisted Spark

Anthony DeFilippo¹, Benjamin Wolk^{2*}, Jyh-Yuan Chen³, Robert Dibble⁴ and Yuji Ikeda⁵

¹Abengoa Research, Seville, Spain

²Combustion Research Facility, Sandia National Laboratories, Livermore, CA, USA

³Department of Mechanical Engineering, University of California – Berkeley, Berkeley, CA, USA

⁴Clean Combustion Research Center, King Abdullah University of Science and Technology (KAUST), Thuwal, Saudi Arabia

⁵Imagineering Inc., Kobe, Japan

Abstract

Advanced engines can achieve higher efficiencies and reduced emissions by operating in regimes with diluted fuel-air mixtures and higher compression ratios, but the range of stable engine operation is constrained by combustion initiation and flame propagation when dilution levels are high. An advanced ignition technology that reliably extends the operating range of internal combustion engines will aid practical implementation of next-generation high-efficiency engines. The microwave-assisted spark plug under development by Imagineering, Inc. of Japan has previously been shown to expand the stable operating range of gasoline-fueled engines through plasma-assisted combustion, but the factors limiting its operation were not well characterized. The present experimental study has two main goals: (1) to investigate the capability of the microwave-assisted spark plug towards expanding the stable operating range of wet-ethanol-fueled engines, and (2) to examine the factors affecting the extent to which microwaves enhance ignition processes. The stability range is investigated by examining the coefficient of variation of indicated mean effective pressure as a metric for instability, and indicated specific ethanol consumption as a metric for efficiency. Engine efficiency improved when the engine was run at slightly-lean air-fuel ratios, with the onset of instability eventually eliminating efficiency gains associated with lean-burn when mixtures become too dilute. Microwave-assisted ignition reduced dilution-triggered instability, improving efficiency compared to unstable spark-only operation at ultra-lean conditions. Microwave-assisted spark also promotes faster average early flame kernel development when un-enhanced flame kernel development is sufficiently slow. Correlations between microwave-assisted flame development enhancement and calculated in-cylinder parameters suggest a relation between enhancement and the amount of energy deposited into the flame kernel, but scatter prevented derivation of a unifying empirical correlation governing all tested cases.

Keywords: Microwave; Spark; Ethanol; Stability; Dilution

Introduction

Future high-efficiency engines may require the ability to ignite a mixture under conditions where current spark ignition systems are insufficient [1,2]. It has long been known that up to a certain point, dilution of the fuel-air mixture with excess air (lean-burn) or exhaust gas recirculation (EGR) increases an engine's fuel efficiency and decreases emissions [3]. It is also well-documented that further dilution eventually destabilizes combustion such that cycle-to-cycle variations make engine operation impractical.

Destabilization occurs because flame propagation speeds and mixture ignitability decline, leading to the onset of partial-burn and misfire [4]. Thus, at the lean operation limit of a spark-ignited engine, advancing ignition timing will increase occurrence of misfire while retarding ignition timing will increase occurrence of partial-burn. Partial-burn occurrence can be reduced by enhancing flame propagation speed. Turbulence can enhance flame speeds within the combustion chamber, but can adversely affect the ignitability of mixtures [5]. Fuel mixture blending with hydrogen enhances flame propagation rates in lean methane-air mixtures [6], but blending hydrogen with liquid fuels such as gasoline presents its own commercial feasibility challenges.

Another approach to reduce partial-burn cycles at dilute engine operating conditions is to use an advanced ignition system. Past high-energy ignition systems have produced faster burns and more-reliable ignition, leading to efficiency improvements by extending stable operating ranges of internal combustion engines into more-efficient

regimes such as those with higher dilution (air or exhaust gas), higher turbulence, or higher compression ratios. Additionally, plasma-assisted combustion has shown the potential for combustion enhancement through electromagnetic interactions in weakly-ionized reacting gases. Plasma-assisted combustion technologies could translate into a commercially-viable ignition device.

Dale et al. reviewed high-energy ignition strategies that have been investigated for their capability to reduce burn duration and misfire [7]. The authors note that in most production engines, the standard transistor-switched coil spark discharge ignition (spark ignited) systems provide sufficient energy for the ignition of stoichiometric engine mixtures with moderate EGR levels. Durability, cost, and efficiency concerns of novel ignition technologies have prevented their widespread adoption. More-recently, the dual-coil offset ignition technology developed at Southwest Research Institute enabled engine

***Corresponding author:** Benjamin Wolk, Combustion Research Facility, Sandia National Laboratories, Livermore, CA, USA, Tel: 9252946910; E-mail: bmwolk@sandia.gov

Received August 28, 2015; **Accepted** September 30, 2015; **Published** October 10, 2015

Citation: DeFilippo A, Wolk B, Chen JY, Dibble R, Ikeda Y (2015) Stability Limit Extension of a Wet Ethanol-fueled SI Engine using a Microwave-assisted Spark. Adv Automob Eng 4: 123. doi:10.4172/2167-7670.1000123

Copyright: © 2015 DeFilippo A, et al. This is an open-access article distributed under the terms of the Creative Commons Attribution License, which permits unrestricted use, distribution, and reproduction in any medium, provided the original author and source are credited.

operation at higher levels of EGR dilution than a traditional spark engine [8]. The increasingly-studied field of plasma-assisted ignition and combustion presents opportunities for a new generation of ignition technology, and will be discussed in the following section.

Plasma-assisted combustion enhancement

Plasma-assisted combustion research, which investigates combustion enhancement through electromagnetic interactions in gases, has the potential to bring new ignition technologies to market. It has long been known that flames contain charged particles and can be influenced by electric fields [9]. Fialkov [10] provides a comprehensive review of past flame ion measurements and discusses how electric fields can affect flame propagation, flame stabilization, and soot formation. Generation or enhancement of plasma in a combustion environment through the use of microwaves (MW), radio frequency waves (RF), dielectric barrier discharges (DBD), nanosecond discharges, and other electric discharges has been shown to improve ignition characteristics and flame speeds under a variety of conditions and is thus an active area of research, as evidenced by the review by Starikovskaia [11] and later by Starikovskiy et al. [12]. Applications include high-speed scramjet combustion for aerospace applications [13,14] and automotive internal combustion engines [15-21].

Plasmas are commonly categorized as either “thermal” or “non-thermal.” In thermal plasmas, the electron energy is in equilibrium with the energy of the heavy particles, thus characterizing thermal plasmas with high gas temperatures and high levels of ionization. In non-thermal plasmas, energy transferred to electrons can enhance reaction kinetics without causing large increases in translational gas temperatures. Rotational and vibrational gas temperatures can increase and the presence of reactive excited species and radicals can increase the overall rate of reaction in non-thermal plasma, while requiring lower energy input than thermal plasma. Ombrello isolated the chemical effects of combustion enhancement associated with elevated concentrations of Ozone, O_3 [22] from those associated with singlet Oxygen ($O_{2a}^1\Delta_g$) [23]. While most previous studies isolate plasma from the flame so that isolated species or effects can be studied, Sun et al. [24], developed an apparatus for studying extinction limits of low-pressure counter-flow methane diffusion flames directly interacting with a plasma, determining that a nanosecond pulsed electric discharge can change the shape of the ignition-extinction curve from an S-curve to a monotonic extinction/ignition curve.

One method of delivering energy to electrons in gases that has seen considerable research attention is through microwaves. However, previous research concerning microwave enhancement of hydrocarbon flame speed has offered an inconsistent range of observations and explanations for those observations. Groff et al. [25] measured flame speed enhancements that they attributed primarily to local microwave heating of gases. Clements et al. [26] also measured significant flame speed enhancement of hydrocarbon flames, but only at the lean limit and under electrical breakdown conditions, concluding that microwave enhancement of flames is impractical due to the high energy requirements. Shibkov [13] employed freely localized and surface microwave discharges for generating plasma in supersonic airflow and for igniting supersonic hydrocarbon fuel flows. Stockman et al. [14] employed a pulsed microwave delivery strategy that reduced the energy requirement and measured up to 20% enhancement of flame speed in hydrocarbon flames, with measurements suggesting that chemical effects were likely responsible for this enhancement [14]. Michael [27] and Wolk [28] coupled spark breakdown with microwave input in quiescent fuel-air mixtures. Sasaki [29] measured enhanced burning

velocities of premixed methane-air flames in a burner subject to pulsed microwave irradiation, attributing the enhanced reactivity to energetic electron interactions since gas temperature increases were negligible.

Wet ethanol as a fuel with potential life-cycle energy savings

Motivation for studying internal combustion engine operation with ethanol-water mixtures as a fuel comes from the potential for life-cycle energy savings. Ethanol, a bio-fuel compatible with an increasing number of road vehicles, is often criticized for the high energy cost of its production. Production of 100% pure, fuel-grade ethanol requires water removal through dehydration and distillation processes that demand an energy input equivalent to 37% of the energy content of the fuel [30]. Analysis shows that direct use of “wet-ethanol” that is 35% water by volume reduces the energy cost of dehydration and distillation to 3% of the fuel energy content [30]. An example of the energy savings for wet ethanol is illustrated in Figure 1. Wet ethanol has previously been demonstrated as a fuel in Homogeneous Charge Compression Ignition (HCCI) engine operation with water dilution up to 60% water (40% ethanol) by volume [31]. Unfortunately, ethanol fuel with water content greater than 0.5% by weight carries ions that accelerate corrosion of the fuel system [32], so practical implementation of wet-ethanol as a fuel will require advances in fuel system metals or treatments. Nonetheless, the present parametric study of engine performance with diluted ethanol fuel presents a fundamental dataset for understanding microwave-assisted spark plug performance under a range of operating conditions.

Present study of plasma-assisted ignition in a wet ethanol-fueled engine

This paper analyzes the capabilities of a microwave-assisted spark plug through analysis of a multi-parameter test matrix completed in an ethanol-fueled single-cylinder Waukesha ASTM-Cooperative Fuel Research (CFR) engine under varied conditions, notably increased compression ratio, increased preheat, and increased charge dilution. Independent variables include compression ratio (9:1, 10.5:1, and 12:1); fuel water dilution by volume (0%, 20%, 30%, 40%); intake air temperature (22°C, 60°C); air/fuel ratio (stoichiometric to lean-stability-limit); spark timing (advanced, maximum brake torque, retarded); and ignition strategy (spark only, spark with microwave).

This paper demonstrates the extension of the stable engine operating

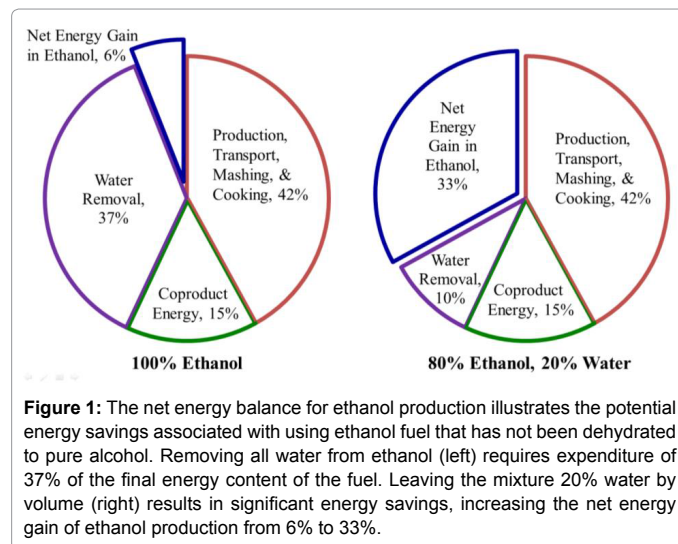


Figure 1: The net energy balance for ethanol production illustrates the potential energy savings associated with using ethanol fuel that has not been dehydrated to pure alcohol. Removing all water from ethanol (left) requires expenditure of 37% of the final energy content of the fuel. Leaving the mixture 20% water by volume (right) results in significant energy savings, increasing the net energy gain of ethanol production from 6% to 33%.

range by a microwave-assisted spark plug, with data indicating that microwave-assisted spark ignition reduces cyclic variation as compared to spark-only ignition in highly-dilute mixtures at all tested compression ratios and intake air temperatures. Examination of the factors affecting microwave ignition performance shows diminished effects of microwave energy input when in-cylinder pressures are high at time of spark.

Experimental Apparatus and Data Acquisition

The present experimental study has two main goals: the first goal is to investigate the capability of a microwave-assisted spark plug towards expanding the stable operating range and improving efficiency of wet-ethanol-fueled engines, which is conducted through examination of the coefficient of variation of indicated mean effective pressure and the indicated specific ethanol consumption. The second goal is to examine the factors determining the effectiveness of microwaves in enhancing ignition processes. Factors affecting microwave enhancement of ignition processes are individually examined, using flame development behavior as a key metric in determining microwave effectiveness.

Engine apparatus

A single-cylinder Waukesha ASTM-Cooperative Fuel Research (CFR) engine is employed in the present engine testing. A schematic of the engine system and associated sensors is presented in Figure 2 with engine specifications listed in Table 1. Intake air comes from an in-house air compressor regulated to 99 ± 0.5 kPa and is passed through a controlled heater and an intake plenum. Intake temperatures in the present study range from 18.2°C to 87.4°C. Engine speed is maintained at 1200 rpm for all tests. Engine coolant temperature is controlled at 75°C. A MoTeC M4 Engine Control Unit (ECU) controls ignition timing, fuel injection pulse width, and fuel injection duty cycle. The engine is fueled with mixtures of pure ethanol and distilled water delivered through a nitrogen-pressurized fuel system.

Displacement	0.616 L
Stroke	114.3 mm
Bore	82.804 mm
Connecting Rod	254 mm
Number of Valves	2
I VO @ 0.15 mm lift	-343°C _A ATDC _{compression}
I VC @ 0.15 mm lift	-153°C _A ATDC _{compression}
E VO @ 0.15 mm lift	148°C _A ATDC _{compression}
E VC @ 0.15 mm lift	-353°C _A ATDC _{compression}
Engine Speed	1200 RPM
Compression Ratio (CR)	9:1, 10.5:1, 12:1

Table 1: Cooperative Fuel Research (CFR) engine specifications.

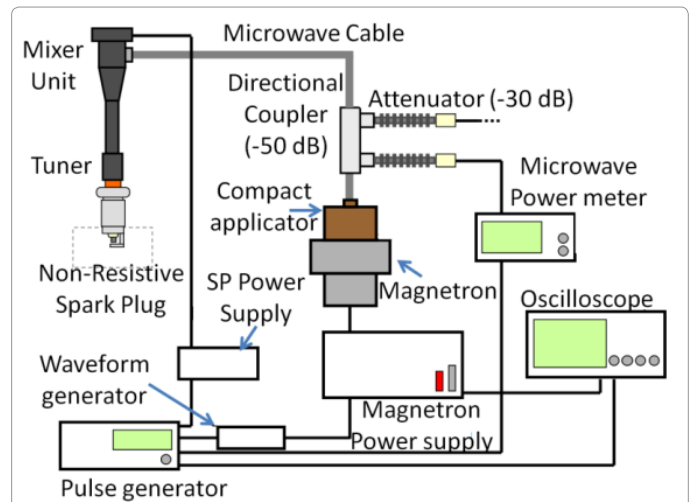


Figure 3: Schematic of microwave-assisted spark system provided by Imagineering, Inc.

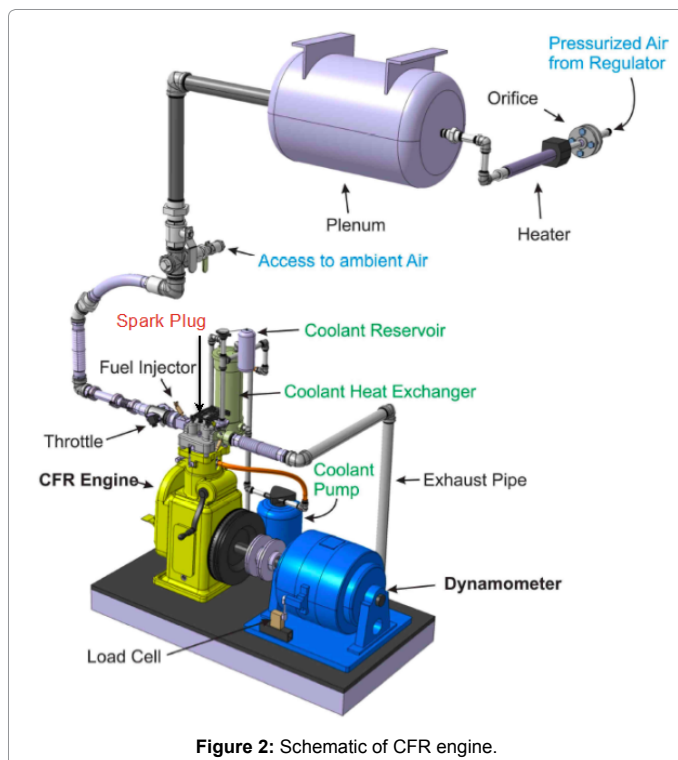


Figure 2: Schematic of CFR engine.

Microwave-assisted ignition system

The air-fuel mixture is ignited using a prototype microwave-assisted spark plug system developed by Imagineering Inc. [15-16], which couples microwave emission to a standard spark discharge typical of current automotive engines. The ignition system can be operated with and without microwave assist. A standard spark is delivered via a discharge implementing a 1000 μF capacitor and an automotive ignition coil, initiating plasma in the combustion chamber through DC breakdown across a NGK BP6ES spark plug. Along with the spark, 2.45 GHz microwaves generated by a magnetron from a commercially-available microwave oven are directed through the spark plug insulator and into the combustion chamber. The microwaves transfer energy to the free electrons generated in the initial spark plasma and flame kernel. A schematic of the ignition system is shown in Figure 3.

Pulsed power input to the magnetron has a peak power of 2.6 kW with about 500 W average power. Power is pulsed to the magnetron at a 25% duty cycle: “on” for 4 μs followed by 12 μs “off.” The total microwave energy input can be varied by modifying the total duration of the energy input pulse train, but the amplitude of energy input is not presently adjustable. For the current tests, microwave input duration is set to 2.5 ms per spark event. Because of microwave reflection, transmission losses, and magnetron inefficiencies, the microwave power delivered to the spark zone is about 20% of the power consumed by the magnetron (i.e. 80% loss). Reflected microwaves are measured using a 50 dB directional coupler. The microwave is started 0.25 ms

before spark initiation, with a total duration of 2.5 ms, corresponding to a microwave energy input to the combustion chamber after spark initiation of about 220 mJ. A timing diagram is presented in Figure 4. The microwave spark system is tuned to minimize measured reflected microwaves, but the combustion chamber is not optimized towards promoting constructive interference of microwaves.

The microwave-assisted spark plug under development by Imagineering Inc. used in this study initiates plasma using a standard spark discharge from an ignition coil, then enhances electron energy and expands the plasma by emitting microwaves into the combustion chamber. Microwaves generated by a magnetron at a frequency of 2.45 GHz are transmitted through the spark plug insulator into the combustion chamber. In the combustion chamber, microwaves are absorbed by the free electrons in the spark discharge, generating non-thermal plasma. The Imagineering Inc. microwave-assisted spark plug cannot generate plasma without first initiating a spark discharge, indicating that the subcritical microwaves do not create plasma simply by a coronal discharge between the conducting spark plug electrode and the ground [15]. Electric field simulations by the designers of the microwave spark plug system in a 75 mm diameter × 130 mm cylindrical chamber estimate the maximum electric field strength, concentrated at the electrode, as approximately 2000 V/m, with field strength attenuating approximately by the third power of distance from the spark plug electrode [33], a decay rate perhaps relating to the exponential Bouger law decay of an electromagnetic wave propagating into a plasma [34]. The rapid attenuation of microwave power with distance from the electrode implies that as the flame front grows away from the electrode, there is little microwave energy remaining which can be coupled into the flame front. The benefits of microwave assist are thus only realized in the early stages of combustion when the flame kernel is still near the spark electrode. The designers of the microwave-assisted spark system also spectroscopically measured high levels of OH radicals during the microwave discharge event, concluding that electron-impact reactions with water molecules in the microwave plasma increase the pool of oxidizing radicals, enhancing the early stages of combustion through chemical effects [15].

Data acquisition

Engine performance is evaluated on the basis of in-cylinder pressure and exhaust gas measurements. Cylinder pressure is measured using a 6052B Kistler piezoelectric pressure transducer, with signals amplified by a 5044A Kistler charge amplifier. The cylinder pressure

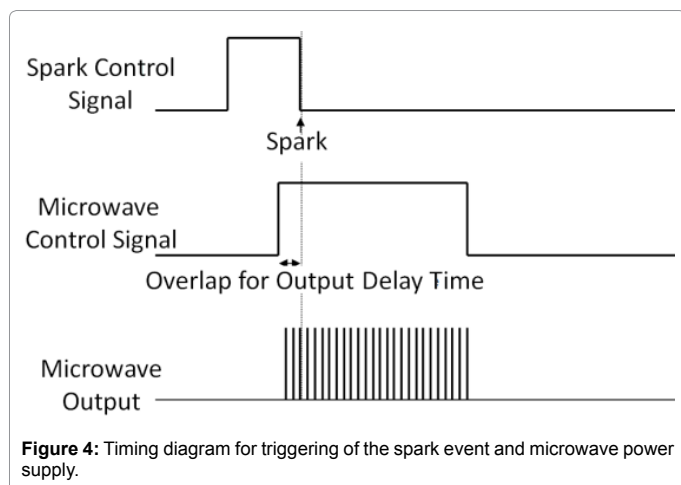


Figure 4: Timing diagram for triggering of the spark event and microwave power supply.

Compression Ratio	Fuel mix by volume	T _{intake}	Air-fuel ratio (λ)	Ignition Mode	Spark Timing
9:1	100% Ethanol	22 °C	Stoichiometric	Spark-Ignited Only	Advanced ↓ Maximum Brake Torque
10.5:1	80% Ethanol				
12:1	70% Ethanol	60 °C	↓ Lean	Microwave-Assisted Spark	↓ Retarded
	60% Ethanol				

Table 2: Experimental conditions.

transducer is mounted in an extra spark plug hole in the cylinder head. For each operating condition, 200 cycles of in-cylinder pressure data are recorded, with data measured every 0.1 crank angle degree (°CA). Intake pressure is measured using a 4045A5 Kistler piezoresistive pressure transducer, with signals amplified by a 4643 Kistler amplifier module. Crank angle position is determined using an optical encoder, while an electric motor controlled by an ABB variable speed frequency drive controls the engine speed.

Exhaust gas composition is measured for determination of air-fuel ratio and pollutant production. Exhaust gas is sampled downstream of the exhaust port. Water is condensed from the sample line, and the sample is sent to a Horiba gas analyzer. The gas analyzer measures concentrations of unburned hydrocarbons, oxygen, carbon monoxide, carbon dioxide, and nitric oxides (NOx). Each gas analyzer is calibrated with a “zero gas” (nitrogen) and a “span gas” of known concentration.

The experimental test matrix is summarized in Table 2 below. Tests were run at three values of compression ratio (CR): 9:1, 10.5:1, and 12:1; four mixtures of ethanol and water: 100%, 80%, 70%, and 60% ethanol by volume; two target intake temperatures (T_{intake}): 22°C and 60°C; a range of air-fuel mixtures from near stoichiometric to lean stability limit; and two ignition modes: microwave-assisted spark and spark-ignited only. Additionally, spark timing was varied to find maximum-brake-torque conditions and for investigation of microwave effects with advanced and retarded timing.

Raw measurements of intake pressure, in-cylinder pressure, intake temperature, and exhaust gas concentration must be converted to more-useful parameters for an in-depth analysis of the combustion processes of interest. The following subsections discuss the methods for calculating the engine parameters of interest.

For a fuel of general formula C_αH_βO_γ, here ethanol, C₂H₆O, the normalized air-fuel ratio, λ, is estimated by assuming complete combustion and using the measured exhaust gas concentrations of oxygen, [O₂], and carbon dioxide, [CO₂], as in Eq. 1.

$$\lambda = 1 + \frac{\alpha}{\alpha + \frac{\beta}{4} - \frac{\gamma}{2}} \frac{[\text{O}_2]}{[\text{CO}_2]} = 1 + \frac{2}{3} \frac{[\text{O}_2]}{[\text{CO}_2]} \quad (1)$$

Air-fuel ratio calculated from exhaust gas measurements using Eq. 1 correlates with the amount of pure ethanol injected divided by the normalized mass of air inhaled, inferred from measurements of intake manifold temperature and pressure. For each ethanol-water mixture, a correlation was developed so that air-fuel ratio could be

determined even when exhaust gas measurements were unreliable due to instabilities and incomplete burning.

Calculating engine output, stability, and efficiency

Engine output is determined using indicated mean effective pressure (IMEP). IMEP is calculated from the recorded pressure trace for each of 200 consecutive cycles using Eq. 2. Gross IMEP includes work during the compression and power strokes [35].

$$\text{Gross IMEP (bar)} = \frac{\text{Work}}{\text{swept volume}} = \frac{\oint P \times dV}{\text{swept volume}} \quad (2)$$

The coefficient of variation of IMEP (COV_{IMEP}) is a metric for measuring engine instability. COV_{IMEP} is the standard deviation of the set of 200 calculated IMEPs for a given engine condition, σ_{IMEP} normalized by the mean IMEP over the set of 200 consecutive cycles, \bar{x}_{IMEP} , as in Eq. (3). Lower COV_{IMEP} indicates a more stable combustion process; with $\text{COV}_{\text{IMEP}} < 5\%$ desirable and $\text{COV}_{\text{IMEP}} > 10\%$ considered outside the stability limit [35].

$$\text{COV}_{\text{IMEP}} (\%) = \frac{\sigma_{\text{IMEP}}}{\bar{x}_{\text{IMEP}}} \times 100 \quad (3)$$

Fuel consumption is presented in terms of indicated specific ethanol consumption (ISEC), which relates the mass of pure ethanol injected to a unit of indicated work output as in Eq. 4. Mass of fuel injected per cycle is known by calibrating the fuel injector pulse width.

$$\text{ISEC} \left(\frac{\text{g}}{\text{kw} \times \text{hr}} \right) = \frac{\text{mass ethanol injected (g) / cycle}}{\text{work (kw} \times \text{hr) / cycle}} = \frac{\text{mass ethanol (g)}}{\oint P \times dV} \quad (4)$$

Analysis of heat release during the early stages of combustion provides a metric for comparing microwave-assisted ignition performance to spark-only ignition. Net heat release rates are calculated from the measured in-cylinder pressure (P) history and known volume (V) history for each engine cycle using Eq. 5. Integration of the instantaneous net heat release rate gives a cumulative net heat release rate as a function of engine crank angle.

$$\frac{dQ_{\text{net}}}{d\theta} = \frac{\gamma(\theta)}{\gamma(\theta)-1} P \frac{dV}{d\theta} + \frac{1}{\gamma(\theta)-1} V \frac{dP}{d\theta} \quad (5)$$

The cylinder volume as a function of crank position is determined using the slider-crank formula [35], with engine parameters (bore, stroke, compression ratio, and connecting rod length) listed in Table 1. Q_{net} is the difference between heat released from combustion and wall heat losses. The ratio of specific heats, $\gamma(\theta, \lambda, f_{\text{burned}})$, is calculated based on mixture conditions and temperature using the code discussed in the next section as a function of crank angle position, θ , air-fuel ratio, λ , and combustion progress, f_{burned} , assuming linear progress from an unburned mixture to a burned mixture between time-of-spark and experimental peak-pressure location.

Analysis of heat release during the early stages of combustion provides insight into the benefit of microwave enhancement at the lean stability limit. Since partial burning is strongly to blame for the instability and lost efficiency observed at lean conditions, it is helpful to examine the effects of microwave addition on heat release. “Flame development time,” defined as the time elapsed between spark initiation and 10% of cumulative net heat release [35], provides insight into the early stages of combustion. The time delay between 10% of cumulative net heat release and 90% cumulative net heat release is here called the “flame rise time.” Figure 5 shows the flame development time and flame rise time on a plot of cumulative net heat release calculated

from engine pressure data for a single cycle.

Calculating in-cylinder properties

An implementation of the slider-crank formula [35] in Cantera [36] simulates mixture evolution inside a compressing piston by integrating the energy conservation equation for a gas mixture subject to a crank-angle-dependent volume, allowing estimation of not-easily-measured parameters such as in-cylinder temperature and specific heat ratio as a function of crank angle and the experimental conditions which serve as the initial conditions for the model.

The energy equation takes the form of a differential equation for in-cylinder temperature, T, as in Eq. 6. The first term accounts for compression work, $P \times \frac{dV}{dt} \sim \frac{J}{s}$. The second term accounts for net species internal energy change from chemical reactions, with $\dot{\omega}_i \sim \frac{\text{mol}}{\text{cc} \times \text{s}}$ the net formation rate of chemical species i,

$U_i(T) \sim \frac{J}{\text{mol}}$ the internal energy of species i at temperature T, and $V(t) \sim \text{cc}$ the in-cylinder volume at time t. The third term accounts for wall heat losses, $\dot{Q}_{\text{loss,wall}} \sim \frac{J}{s} = h(T, P) \times A(t) \times (T - T_{\text{wall}})$, modeled using the Woschni model [37], with $A(t) \sim \text{m}^2$ the cylinder wall area, and $h(T, P) \sim \frac{W}{\text{m}^2 \times K}$, the instantaneous heat transfer

coefficient, proportional to $P^{0.8} T^{0.53}$ and a constant factor tuned for agreement between predicted and experimental pressure history of motored engine cycles at the various compression ratios and intake air temperatures employed in the present study. The denominator of the energy equation includes the mixture density $\rho \sim \text{kg/m}^3$, the cylinder volume $V(t) \sim \text{m}^3$, and the average mixture heat capacity, $\bar{C}_v \sim \frac{J}{\text{kg} \times K}$.

At each time step of the calculation, Cantera calculates the specific heat ratio of the unburned mixture, $\gamma = c_p / c_v$.

$$\frac{dT}{dt} = \frac{-P \times \frac{dV}{dt} - V(t) \times \sum_{i=1}^{n_{\text{species}}} \dot{\omega}_i U_i(T) - \dot{Q}_{\text{loss,wall}}}{\rho \times V(t) \times \bar{C}_v} \quad (6)$$

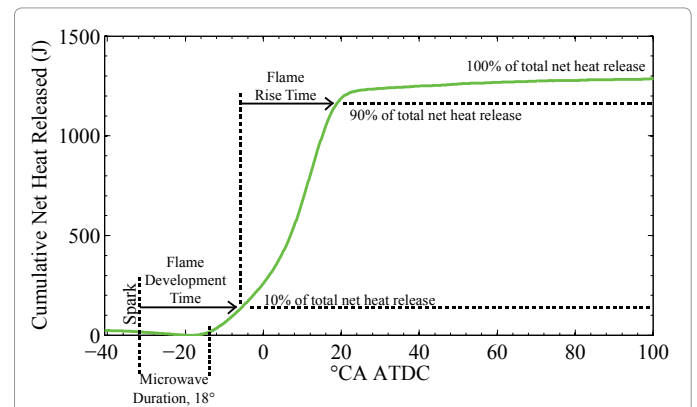


Figure 5: Cumulative net heat release calculated for a single engine cycle from pressure data collected at 1200 RPM. The “Flame Development Time” is the time from spark initiation to 10% of cumulative net heat release. The “Flame Rise Time” is the time from 10% to 90% cumulative net heat release. The microwave input duration of 18°CA is shown for illustration.

Once the simulated piston reaches top-dead-center (TDC), the unburned temperature at TDC, which has increased from the initial temperature due to compression heating, is recorded as the “unburned temperature at top-dead-center,” as well as the unburned gas specific heat ratio, γ_{unburned} . A chemical equilibrium calculation beginning with the gas mixture in its TDC condition, holding enthalpy and pressure constant, finds the constant-pressure adiabatic flame temperature, referenced as the “burned temperature at top-dead-center,” as well as the burned gas specific heat ratio, γ_{burned} . The unburned and burned TDC temperatures define the regime diagram as will be discussed in Section 3.1 for consistency with the procedure of generating a regime diagram by Lavoie et al. [38].

Results and Discussion

The following subsections present an analysis of the large amount of experimental data collected and diagrammed in Table 2 with a narrowing focus. First, the practical considerations of the microwave-assisted spark are considered: analysis focuses on the extent to which microwave-assist expands the stable operating range of a wet-ethanol-fueled engine as compared to standard spark ignition operation. Next, the focus narrows to an analysis of burn characteristics, with data showing that microwave assist enhances early heat release rates under certain conditions of engine operation. Finally, the factors contributing to microwave effectiveness are explored through isolation of specific variables and analysis of their impact on microwave effectiveness.

Extension of the stable operating range

A main goal of this study is to investigate the possibility of extending the stable operating range of a spark-ignited engine with wet-ethanol as a fuel. The fuel compositions, air-fuel mixtures, and intake temperatures span a wide range of operating modes. The multi-mode combustion diagram of Lavoie et al. which delineates the possible regimes of internal combustion engine operation, is a useful tool for visualizing a large range of engine modes [38]. Operating points of the multi-mode combustion diagram are described by the unburned and burned gas temperatures at top-dead-center. The unburned and burned gas temperatures for a given operating point depend on the compression ratio, the fuel mixture, the intake air temperature, and the air-fuel ratio. With operating conditions defining initial conditions and engine geometry, the procedure discussed in the previous section solves for unburned and burned gas temperatures for each experimental condition. Conditions with higher intake temperatures and higher compression ratios will have higher unburned temperatures at TDC. Conditions with high charge dilution, whether by water-fuel mixing or air dilution (lean-burn) have lower burned temperatures at TDC due to increased mixture heat capacity relative to the amount of fuel injected, and thus a reduced adiabatic flame temperature.

All experimentally-measured stable engine operating points ($\text{COV}_{\text{IMEP}} < 10\%$) are plotted on the regime diagram in Figure 6 for both ignition modes: spark-only and microwave-assisted ignition. The operating points exhibiting stable operation are connected in planes, with the plane for microwave-assisted spark operation extending into regions with lower “burned” temperatures than the plane of the spark-ignited-only mode. Extension into regions with lower “burned” temperatures indicates that the microwave-assisted spark mode allows stable engine operation in mixtures with higher dilution and a corresponding lower flame temperature. Stability limit extension by microwave-assisted spark occurs over all “unburned” temperatures, indicating that the microwave-assisted spark effectively extends stability limits even with high intake temperatures and high compression ratios.

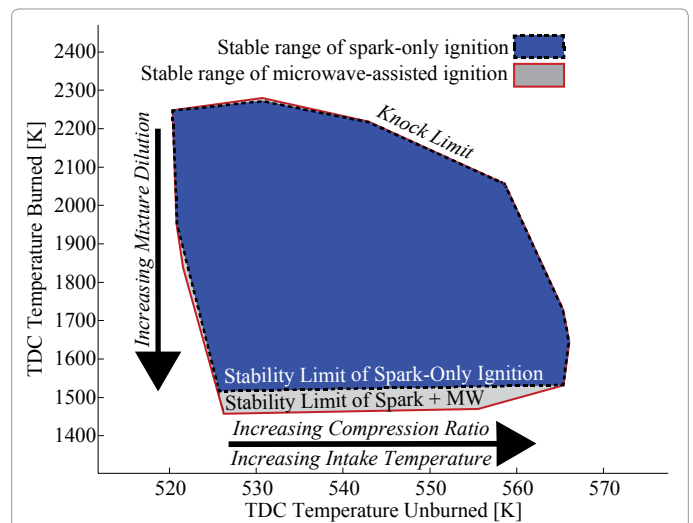


Figure 6: Regime diagram of engine operation showing that microwave-assisted spark allows stable engine operation ($\text{COV}_{\text{IMEP}} < 10\%$) in a larger range than possible with spark ignition only. Microwave assist extends stable engine operation into regimes with lower flame temperatures (increased charge dilution).

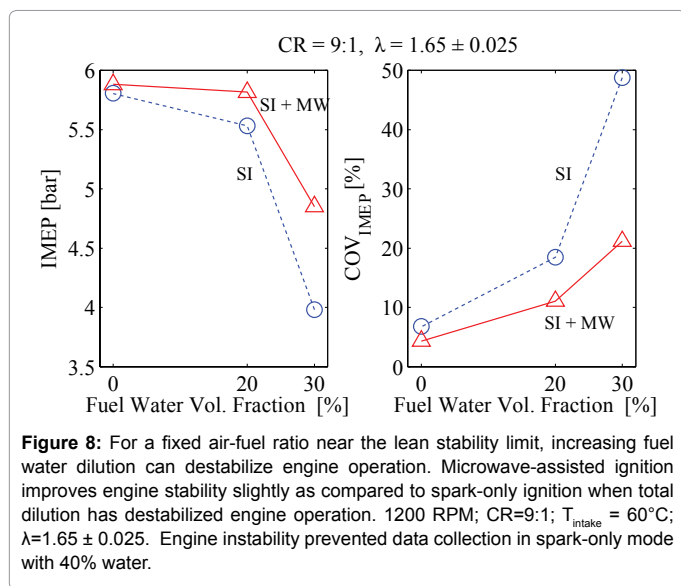
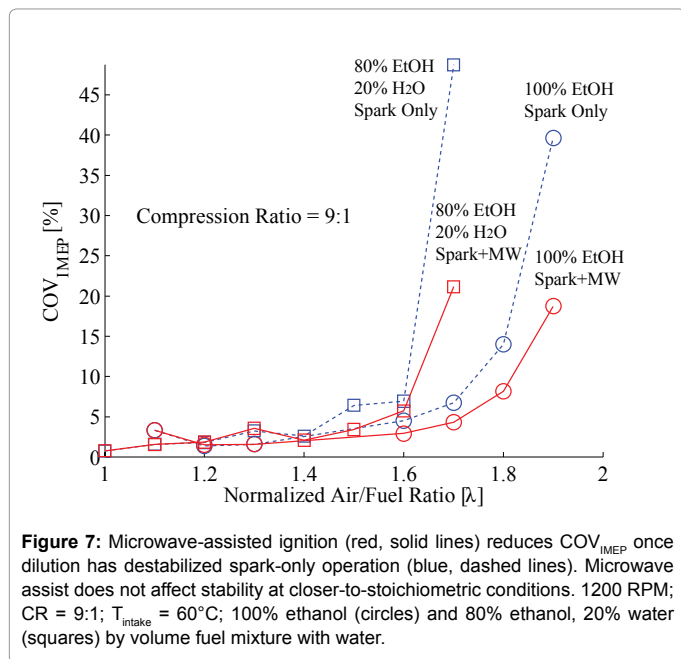
Microwave extension of the stability limit diminishes at the highest unburned gas temperatures.

Extension of stability range

Though the regime diagram concisely demonstrates an overall extension of the stable operating range by the microwave-assisted spark mode, it does not indicate whether the instabilities overcome by the microwave-assisted mode are due to charge dilution with air or fuel dilution with water. The remainder of this section presents examples suggesting that the microwave-assisted spark plug is effective in counteracting instability caused by both air dilution and water dilution.

At a given engine condition (fixed CR, T_{intake} , fuel type, and engine speed), reducing the mass of fuel injected per cycle from stoichiometric conditions increases the air-fuel ratio (lean), eventually leading to engine instability as indicated by a high COV_{IMEP} . Figure 7 shows destabilization of lean engine operation in terms of COV_{IMEP} vs. λ at CR = 9:1 and $T_{\text{intake}} = 60^\circ\text{C}$, with 100% ethanol fuel (W0) and 80% ethanol/20% water (W20) by volume fuel. For both fuel types, the engine is stable at nearer-stoichiometric conditions, $\lambda < 1.5$, and the microwave-assisted ignition mode does not improve engine stability. As the air-fuel ratio increases, engine operation destabilizes, with COV_{IMEP} of the spark-only ignition mode increasing outside of the stable range. Both fuel mixtures destabilize, but the greater water dilution of the W20 case causes destabilization at a lower air-fuel ratio. Addition of microwave energy to the ignition event reduces COV_{IMEP} at high air-fuel ratios, improving stability.

In addition to improving stability when engine operation has been destabilized by air dilution, the microwave-assisted spark ignition mode can improve stability when engine operation is destabilized by water dilution of the fuel. The engine was run with a constant amount of pure ethanol injected per cycle, with varied amounts of water dilution mixed with the fixed amount of ethanol. Comparison of engine data with a fixed mass of ethanol injected per engine cycle (42 mg) and varied amounts of water dilution in Figures 8 and 9 show that water dilution can destabilize engine output, increasing COV_{IMEP} to unacceptable

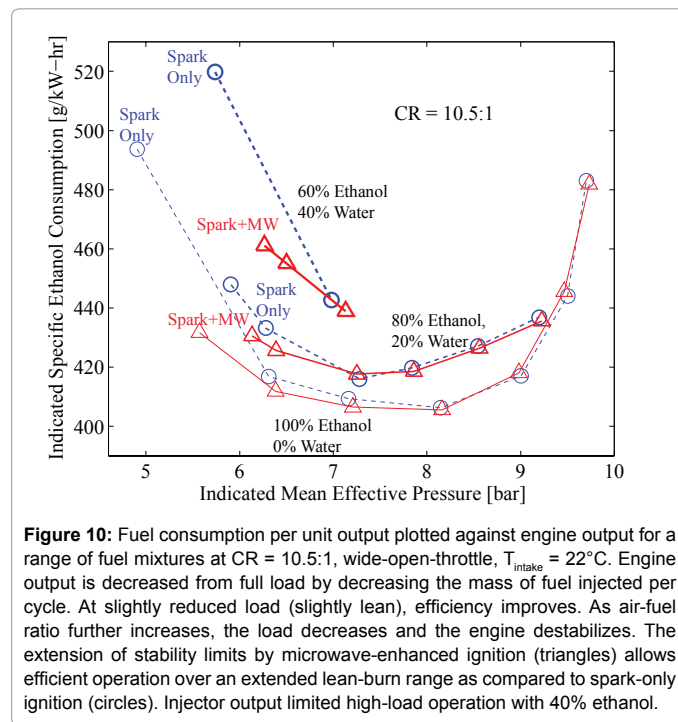
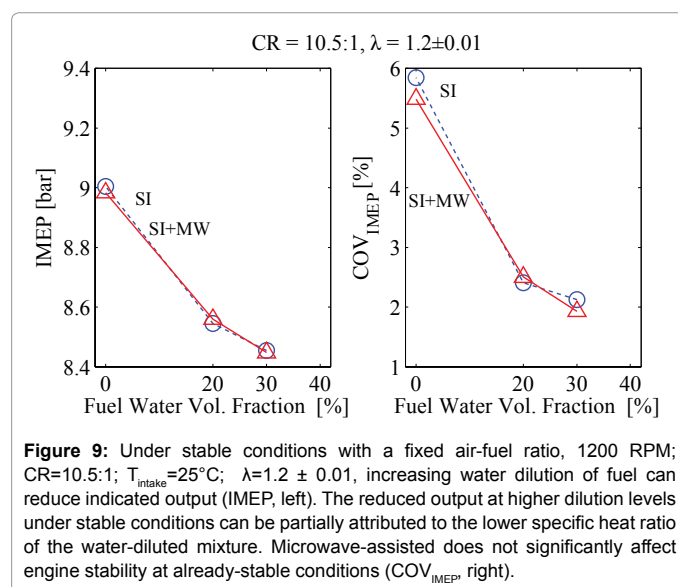


levels. Water dilution decreases engine output if instabilities limit complete burning. Reduced output is attributable to the unstable operation and the higher mixture heat capacity. Microwave-assisted ignition improves stability, resulting in increased average power input as compared to unstable operation in the spark-only ignition mode.

Effect of microwave input on engine efficiency

Since the main motivation for the present undertaking is the improvement of energy efficiency, it is important to examine the effect of stability limit extension on efficiency. Figure 10 plots indicated specific ethanol consumption (ISEC), an inverse measure of efficiency, against engine output for a range of fuel mixtures and air-fuel ratios. Engine output decreases from full load by decreasing the mass of fuel injected per cycle such that the engine enters lean-burn mode. At slightly lean conditions, efficiency improves. As air-fuel ratio increases

and the engine destabilizes, efficiency drops as an increased frequency of partially-burning cycles leaves some fuel unburned. Microwave enhancement mitigates the instability at low-load conditions, reducing the efficiency fall-off of by reducing the frequency and severity of partial burn cycles. The reduction of partial-burn cycles using microwave-assist increases the IMEP level compared to spark-only for the lowest load points. The extension of stability limits by microwave-enhanced ignition allows efficient operation over an extended lean-burn range as compared to spark-only ignition. However, the greatest overall efficiency is not achieved due to lean-limit extension, as the improvements of stability by microwaves at lean-burn conditions do not fully eliminate the occurrence of partial-burn cycles.



The lowest indicated specific fuel consumption for each compression ratio, fuel mixture, and intake temperature tested in the present study gives insight into conditions under which the currently-tested microwave-assisted ignition system can improve efficiency as compared to spark-only operation. Best ISEC points are plotted in Figure 11 for intake temperature of 60°C and in Figure 12 for intake temperature of 22°C. At typical combinations of engine geometry, air temperature, and fuel/water mixture, the most-efficient air-fuel ratio is stable under both microwave-assisted (MW) and spark-only (SI) ignition modes, so microwave-assist does not improve overall efficiency. When intake temperature and compression ratio are high ($T_{\text{intake}} = 60^\circ\text{C}$, CR = 12:1), the onset of engine knock near stoichiometric conditions requires that the fuel-air mixture be diluted to lean mixtures. As a result, engine operation destabilizes for spark-only ignition for all non-knocking air-fuel ratios. Microwave-assisted ignition improves efficiency under such cases when the most efficient air-fuel ratio is unstable with spark-only ignition. For 40% ethanol cases, engine output was limited by injector output.

Enhanced burning rates by microwave ignition

A faster-developing flame kernel in the early stages of combustion promotes earlier onset of the flame rise stage of heat release between 10% of cumulative net heat release and 90% of cumulative heat net release [35]. An earlier flame rise period will burn faster and more-completely than one beginning later, since decreases in cylinder pressure and temperature during the expansion stroke can slow reaction rates. The effect of microwave addition on early heat release thus has important impact on the entire combustion process, despite the fact that microwaves only directly interact with the flame during the early stages of combustion. Previous research with the microwave-assisted spark plug in a gasoline-fueled engine showed that the microwave-assisted ignition mode decreases average flame development time as compared to spark-only ignition at ultra-lean mixtures, but has

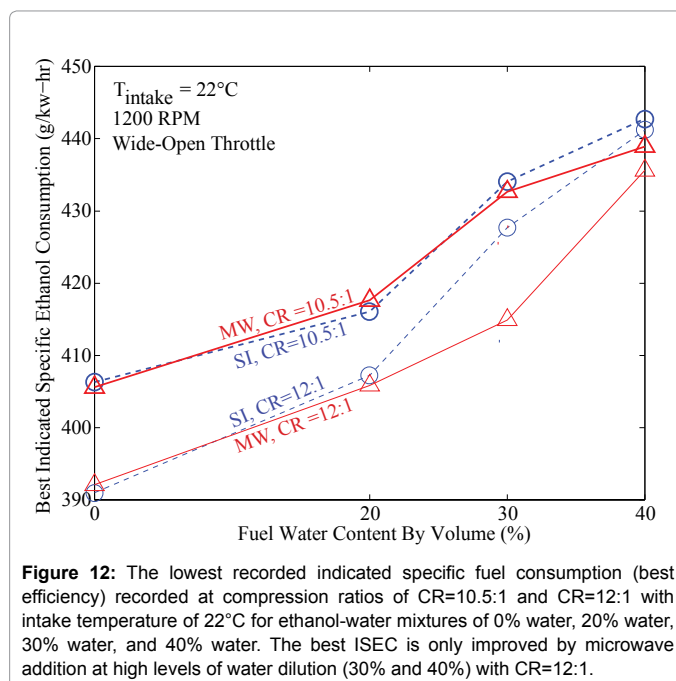


Figure 12: The lowest recorded indicated specific fuel consumption (best efficiency) recorded at compression ratios of CR=10.5:1 and CR=12:1 with intake temperature of 22°C for ethanol-water mixtures of 0% water, 20% water, 30% water, and 40% water. The best ISEC is only improved by microwave addition at high levels of water dilution (30% and 40%) with CR=12:1.

little effect on flame development time at closer-to-stoichiometric mixtures [20]. Figure 13 presents cumulative net heat release curves at two conditions and two microwave input cases, illustrating varied effectiveness of microwave input depending on conditions. At stable, near-stoichiometric operating conditions, microwave input does not significantly affect combustion. At the lean stability limit of a water-diluted fuel, microwave ignition reduces the frequency and severity of partial-burn cycles, improving combustion stability.

Factors influencing microwave effectiveness

The microwave-assisted spark plug has been shown to improve engine stability when air-fuel mixtures are diluted with air or if the fuel is diluted with water, but little benefit is observed when microwaves are added to an already-stable engine mode, an observation that past reports have not explained. In an engine environment, it is difficult to isolate the variables contributing to the observed diminished microwave effects at closer-to-stoichiometric conditions. For example, in a fast-burning, near-stoichiometric fuel-air mixture, the conditions for combustion could simply be strong enough that microwave enhancement is insignificant relative to the unaided burning rate of the spark-ignited mixture. Upon further consideration, the important point may not be that the microwave effects are less relevant when chemistry is faster, but perhaps instead that microwave effects diminish because pressures are higher at the time of spark. A faster-burning mixture requires less burn duration, so the spark is fired closer to top-dead-center. The temperature and pressure are thus higher at time of spark because the spark is initiated later in the compression stroke. The advantage of the present multi-parameter study is that the effects of individual parameters can be studied.

The percent enhancement of flame development time by microwaves will be used in the following subsections as a metric for microwave effectiveness. The percent enhancement by microwaves is determined from the spark-only flame development time (FDT_{SI}) and the microwave-assisted flame development time (FDT_{MW}) using Eq. 7.

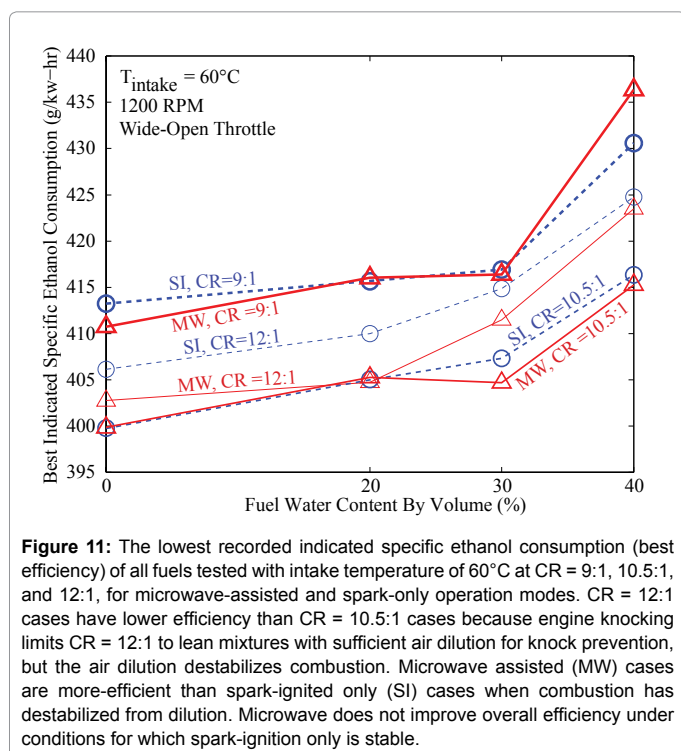


Figure 11: The lowest recorded indicated specific ethanol consumption (best efficiency) of all fuels tested with intake temperature of 60°C at CR = 9:1, 10.5:1, and 12:1, for microwave-assisted and spark-only operation modes. CR = 12:1 cases have lower efficiency than CR = 10.5:1 cases because engine knocking limits CR = 12:1 to lean mixtures with sufficient air dilution for knock prevention, but the air dilution destabilizes combustion. Microwave assisted (MW) cases are more-efficient than spark-ignited only (SI) cases when combustion has destabilized from dilution. Microwave does not improve overall efficiency under conditions for which spark-ignition only is stable.

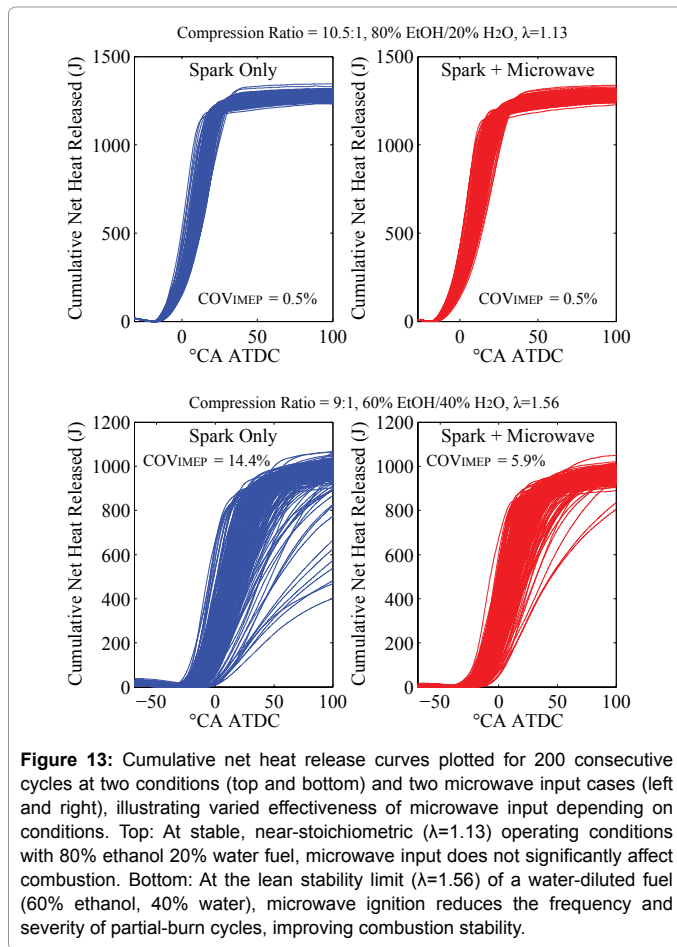


Figure 13: Cumulative net heat release curves plotted for 200 consecutive cycles at two conditions (top and bottom) and two microwave input cases (left and right), illustrating varied effectiveness of microwave input depending on conditions. Top: At stable, near-stoichiometric ($\lambda=1.13$) operating conditions with 80% ethanol 20% water fuel, microwave input does not significantly affect combustion. Bottom: At the lean stability limit ($\lambda=1.56$) of a water-diluted fuel (60% ethanol, 40% water), microwave ignition reduces the frequency and severity of partial-burn cycles, improving combustion stability.

$$\text{Enhancement of FDT by microwaves (\%)} = 100 \times \frac{FDT_{SI} - FDT_{MW}}{FDT_{SI}} \quad (7)$$

Effect of kernel time near the electrode

One potentially important factor determining microwave effectiveness is the time during which the flame kernel is near the spark plug. A slower-developing flame resides near the spark plug longer, allowing more absorbed microwave energy since microwave power attenuates strongly with distance from the plug. Figure 14 plots microwave-assisted flame development time against spark-only flame development time for equivalent engine operating conditions. When combustion is robust and flame development time is short, the addition of microwaves does not accelerate flame development. At longer flame development times, microwaves accelerate flame development relative to spark-only ignition. The observed increased effectiveness of microwave enhancement at longer flame development times may indeed be due in part to the increased amount of time that the flame is near the electrode, but other potentially-important variables such as pressure and temperature at time-of-spark also change as flame development time changes.

Resolving impact of temperature and pressure

Isolating the effects of temperature from the effects of pressure in an internal combustion engine can be difficult because temperature and pressure increase together as the piston compresses the fuel-air mixture before spark. Figure 15 presents a contour plot of FDT enhancement by microwaves against pressure and temperature at

time-of spark for all points with $COV_{IMEP} < 50\%$. The strong coupling between pressure and temperature is apparent by the narrowness of the regime; however there is approximately a 50°C span of temperature at time of spark for each pressure at time of spark. Microwaves most-effectively enhance ignition at low temperature and low pressure, with the strongest enhancement observed only at the lowest pressure. The vertical banding of the enhancement contours implies that pressure is likely more important than temperature in determining microwave effectiveness.

One way to isolate the effects of mixture composition from the effects of mixture pressure and temperature when determining the factors contributing to microwave effectiveness is to vary spark timing from advanced to retarded while holding all other engine conditions constant. Figure 16 shows the results of such an exercise at a CR = 9:1; $T_{Intake} = 60.5^\circ\text{C}$; $\lambda = 2.08$; 80% ethanol 20% water fuel, and 1200 RPM engine speed. When timing is advanced and pressure is low at time-of-spark, microwave ignition significantly enhances flame development time as compared to spark-only ignition. When timing is retarded and pressures are higher at time-of-spark, observed microwave effects

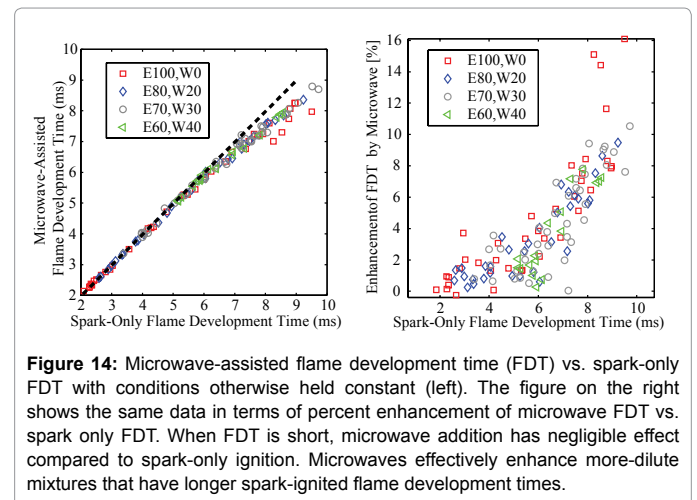


Figure 14: Microwave-assisted flame development time (FDT) vs. spark-only FDT with conditions otherwise held constant (left). The figure on the right shows the same data in terms of percent enhancement of microwave FDT vs. spark only FDT. When FDT is short, microwave addition has negligible effect compared to spark-only ignition. Microwaves effectively enhance more-dilute mixtures that have longer spark-ignited flame development times.

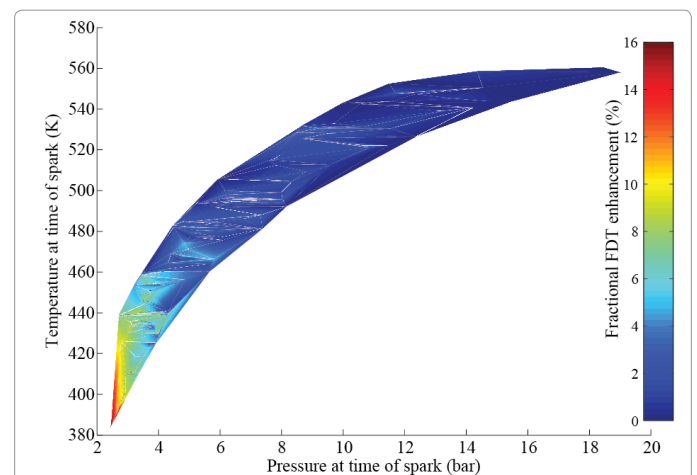


Figure 15: The percent enhancement of FDT by microwaves relative to spark-only FDT is plotted against temperature and pressure at time of spark for all data with $COV_{IMEP} < 50\%$. Microwaves most-effectively enhance ignition at low temperature and low pressure. The strong coupling between pressure and temperature is apparent by the narrowness of the regime.

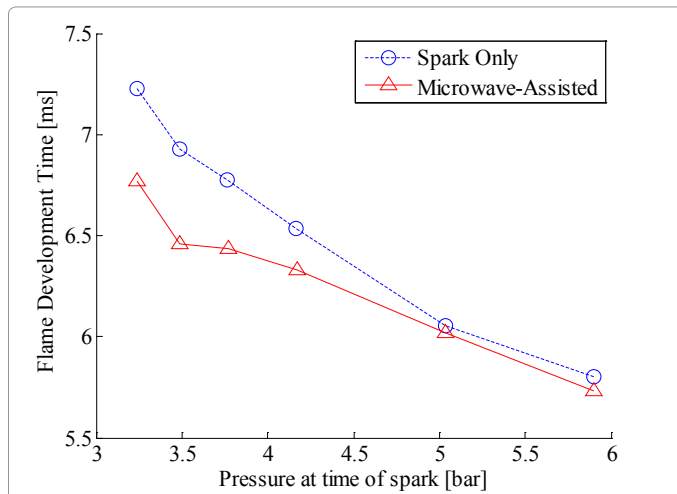


Figure 16: For a fixed engine operating condition (CR =9:1; $T_{\text{Intake}}=60.5^{\circ}\text{C}$; $\lambda=2.08$; 80% Ethanol/ 20% water, 1200 RPM) adjusting spark timing varies the in-cylinder pressure at time of spark. When timing is advanced and pressure low at time-of-spark, microwave ignition strongly enhances flame development time compared to spark-only ignition. When timing is later and pressures are higher at time-of-spark, diminished microwave effects are observed through convergence of flame development times.

diminish, with the microwave-assisted flame development time converging to approximately equal the spark-ignited flame development time. Electron mean free paths in higher-pressure mixtures are shorter, reducing the amount of energy that can be delivered by microwaves to electrons between collisions and thus limiting the possibility for microwave enhancement of chemistry as long as microwave power is held constant.

Correlating microwave enhancement to in-cylinder parameters

Engineering applications will benefit from a better understanding of the physical mechanisms underlying microwave-assisted engine operation, and such understanding can come through correlating microwave effectiveness to in-cylinder properties at time of spark. The state of the art in plasma-assisted combustion suggests that the three main pathways towards plasma enhancement of combustion are thermal, chemical, and transport [1]. Simple theory would then suggest that enhancement by microwaves should relate to the total energy transferred to the mixture by the microwaves, which should be proportional to the time that the flame receives an energy source times the rate of energy input. The energy input rate through joule heating is proportional to the square of reduced electric field $\left(\frac{E}{N}\right)^2$, which is the electric field, E , divided by the gas number density, N [39]. The ideal gas law is here applied for calculating gas number density. Assuming that the microwave source remains on for longer than the flame kernel is near enough to the electrode (within some distance r_{MW}) that it can absorb energy, the time of energy input can be assumed proportional to the inverse of the laminar flame speed, S_L^{-1} , giving a relation roughly proportional to energy coupled into the mixture as in Eq. 8.

$$\text{Energy in} \sim \text{time} \times \text{power} \sim r_{\text{MW}} \times S_{L,E100}^{-1} \times \left(\frac{E}{N}\right)^2 = r_{\text{MW}} \times S_L^{-1} \frac{E^2}{\left(\frac{P}{R_v \times T}\right)^2} \quad (8)$$

For estimating trends in flame speed at time-of spark, the laminar flame speed correlations provided by Bayraktar [40] are applied using the measured in-cylinder pressure at time of spark, P , calculated in-cylinder temperature at time of spark, T_s , and the normalized fuel-air ratio, ϕ as in Eq. 9. The correlation is for pure ethanol only, and in-cylinder turbulence is unknown, so trends in flame speed are here only suitable for comparing trends a fuel mixture with those of that same fuel mixture.

$$S_L(\phi, T, P) = 46.50 \frac{\text{cm}}{\text{s}} \times \phi^{0.25} \times e^{-6.34 \times (\phi - 1.075)^2} \times \left(\frac{T_s}{300 \text{ K}}\right)^{1.75} \left(\frac{P}{1 \text{ bar}}\right)^{-0.17/\sqrt{\phi}} \quad (9)$$

Inverse flame speed, $S_L^{-1}\left(\frac{\text{s}}{\text{cm}}\right)$ is the inverse of the flame speed calculated in Eq. 9, and is used as an estimated factor for correlating in-cylinder conditions with time that the flame kernel is near the spark plug. There is good correlation between the inverse flame speed of a pure ethanol mixture calculated using time-of-spark temperature and pressure and the spark-ignited flame development time (SIFDT) for various ethanol-water mixtures as shown in Figure 17.

Flame speed information for ethanol-water mixtures was unavailable, so flame speed correlations for pure ethanol $S_{L,E100}(T,P,\phi)$, Eq. 9, were applied to all ethanol water mixtures with the understanding that the flame speed correlation will over-predict flame speeds and that the equivalence ratio dependence utilized in the correlation for 100% ethanol may not accurately predict the equivalence ratio dependence of the water-diluted fueling case. Correlations may improve not only through better estimates of flame speed, but also through improvements in calculating in-cylinder heat transfer and mass loss so that in-cylinder temperature can be more-accurately calculated from pressure data using Eq. 6. Figure 18 plots the fractional enhancement of flame development time by microwaves compared to spark-only when microwave energy absorption time is governed by flame speed.

If the flame kernel is near the electrode for a time period greater than the microwave duration, $\text{Duration}_{\text{MW}}$, then the flame speed term will drop out of Eq. 8, and the resulting expression for energy input will be given by Eq. 10. Correlations of microwave enhancement based on equation Eq. 10, are plotted in Figure 19.

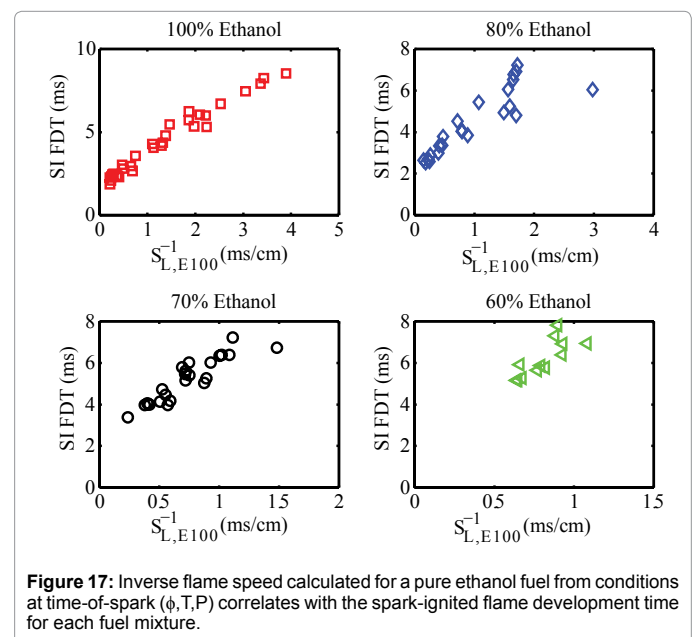
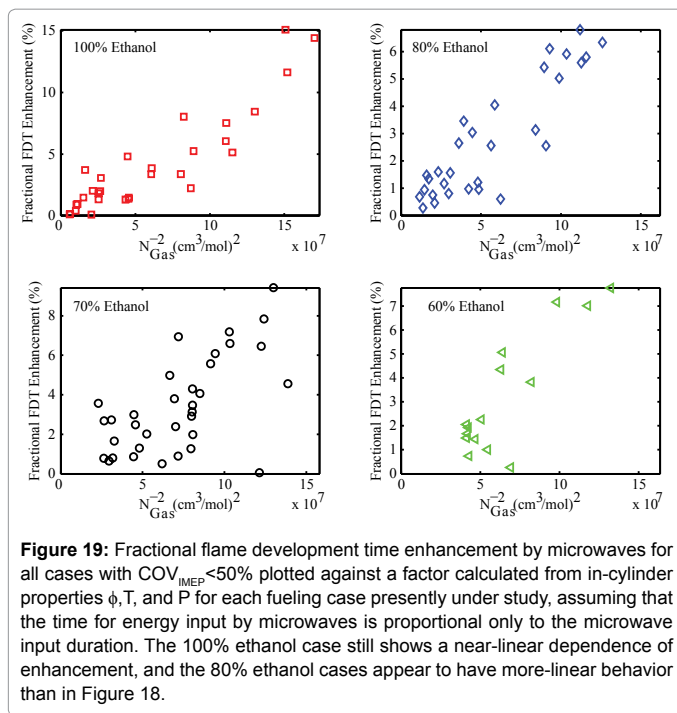
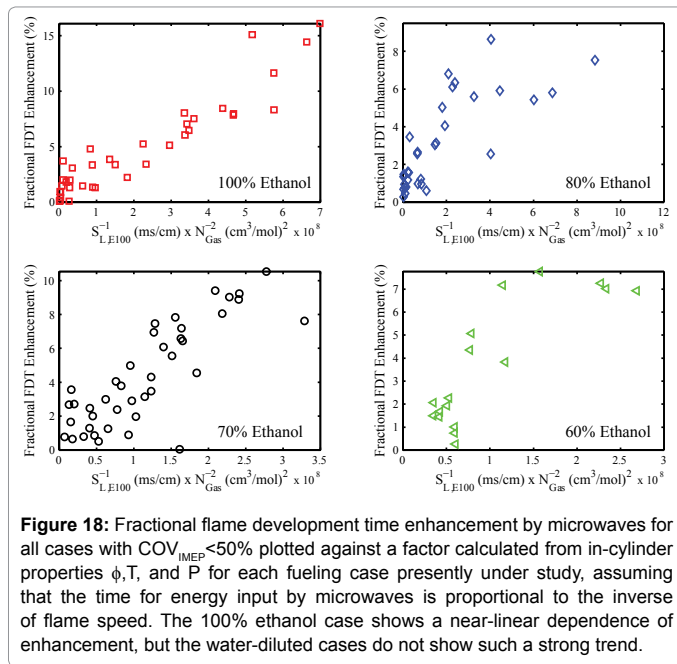


Figure 17: Inverse flame speed calculated for a pure ethanol fuel from conditions at time-of-spark (ϕ, T, P) correlates with the spark-ignited flame development time for each fuel mixture.



$$Energy\ in \sim Duration_{MW} \times \left(\frac{E}{N}\right)^2 = Duration_{MW} \times \frac{E^2}{\left(\frac{P}{R_U \times T}\right)^2} \quad (10)$$

It appears that microwave enhancement of the 80% ethanol case correlates better to energy input when time is assumed proportional to microwave duration (Figure 19, Eq. 10) than when the energy input time is proportional to inverse flame speed (Figure 18, Eq. 8), whereas flame consideration of flame speed may lead to slightly better correlation for the 100% ethanol case. Such a trend may provide

evidence that speed must be considered when predicting microwave effectiveness for faster flames but not slower flames, but on the other hand, scatter in the 70% and 60% ethanol cases makes it difficult to draw definitive conclusions regarding a unifying correlation for microwave enhancement based on in-cylinder conditions at time of spark. The general trend that microwave enhancement of combustion is higher when reduced electric field is higher (lower gas density) does apply to all cases.

Summary and Conclusions

A prototype microwave-assisted spark plug was tested over a range of conditions in a single-cylinder internal combustion engine. The microwave-assisted ignition mode extended stability limits compared to spark-only operation by expanding tolerance to both water dilution of fuel and air dilution of intake charge.

- As expected, engine efficiency improved when the engine was run at slightly-lean air-fuel ratios, with the onset of instability eventually eliminating efficiency gains associated with lean-burn when mixtures become too dilute.

- Microwave-assisted ignition reduced dilution-triggered instability, improving efficiency compared to unstable spark-only operation at ultra-lean conditions.

- Though the more-lean conditions achieved with microwave-assisted ignition have a theoretically higher efficiency, persistence of occasional partial-burn cycles at ultra-lean conditions resulted in the finding that the best overall efficiency achieved by the microwave-assisted spark plug did not exceed the best overall efficiency achieved by spark-only ignition operation.

- Early flame development information deduced from in-cylinder pressure measurements revealed that microwave-assisted spark promotes faster average early flame kernel development when unenhanced flame kernel development is sufficiently slow.

- Isolation of factors contributing to enhancement trends confirmed the importance of mixture pressure on determining microwave-assisted spark effectiveness. Correlations between microwave-assisted flame development enhancement and calculated in-cylinder parameters suggest a relation between enhancement and the amount of energy deposited into the flame kernel, but scatter prevented derivation of a unifying empirical correlation governing all tested cases.

In a practical application, stable operating range extension by microwave-assisted ignition could improve overall efficiency because it could allow a greater range of low-load operation in lean burn mode without throttling losses. Future studies in engines with higher turbulence levels and stratified fuel-air mixtures could provide further insight into the practical applications of microwave-assisted spark.

Acknowledgements

This research at the University of California, Berkeley was partially supported by King Abdullah University of Science and Technology (KAUST), Cooperative Agreement No. 025478 entitled, "Electromagnetically Enhanced Combustion: Electric Flames." The authors would like to acknowledge the efforts of Vi Rapp, Andrew Van Blarigan, Samveg Saxena, and Wolfgang Hable towards the development of the CFR engine experimental platform.

References

1. Ju Y, Sun W (2015) Plasma assisted combustion: Dynamics and chemistry. Progress in Energy and Combustion Science 48: 21-83.
2. Morsy MH (2012) Review and recent developments of laser ignition for internal combustion engines applications. Renewable and Sustainable Energy Reviews 7: 4849-4875.

3. Kuroda H, Nakajima Y, Sugihara K, Takagi Y, Muranaka S (1978) The fast burn with heavy EGR, new approach for low NO_x and improved fuel economy. *SAE Technical Papers* 1-18.
4. Quader AA (1976) What limits lean operation in spark ignition engines-flame initiation or propagation? *SAE Technical Papers* 1-14.
5. Hill PG, Zhang D (1994) The effects of swirl and tumble on combustion in spark-ignition engines. *Progress in Energy and Combustion Science* 20: 373-429.
6. Bell SR, Gupta M (1997) Extension of the lean operating limit for natural gas fueling of a spark ignited engine using hydrogen blending. *Combustion Science and Technology* 123: 23-48.
7. Dale JD, Checkel MD, Smy PR (1997) Application of high energy ignition systems to engines. *Progress in Energy and Combustion Science* 23: 379-398.
8. Alger T, Gingrich J, Mangold B, Roberts C (2011) A continuous discharge ignition system for EGR limit extension in SI engines. *SAE Technical Papers* 1-16.
9. Lawton J, Weinberg FJ (1969) *Electrical aspects of combustion*. Oxford University Press, UK.
10. Fialkov AB (1997) Investigations on ions in flames. *Progress in Energy and Combustion Science* 23: 399-528.
11. Starikovskaia SM (2006) Plasma assisted ignition and combustion. *Journal of Physics D: Applied Physics* 38: R265-R299.
12. Starikovskiy A, Aleksandrov N (2013) Plasma-assisted ignition and combustion. *Progress in Energy and Combustion Science* 39: 61-110.
13. Shibkov VM, Aleksandrov AA, Chernikov VA, Ershov AP, Shibkova LV (2009) Microwave and direct-current discharges in high-speed flow: Fundamentals and applications to ignition. *Journal of Propulsion and Power* 25: 123-137.
14. Stockman E, Zaidi S, Miles R, Carter C, Ryan M (2009) Measurements of combustion properties in a microwave enhanced flame. *Combustion and Flame* 156: 1453-1461.
15. Ikeda Y, Nishiyama A, Wachi Y, Kaneko M (2009) Research and development of microwave plasma combustion engine (Part I: Concept of plasma combustion and plasma generation technique). *SAE Technical Papers* 1-8.
16. Ikeda Y, Nishiyama A, Katano H, Kaneko M, Jeong H (2009) Research and development of microwave plasma combustion engine (Part II: Engine performance of plasma combustion engine). *SAE Technical Papers* 1-8.
17. Tanoue K, Kuboyama T, Moriyoshi Y, Hotta E, Shimizu N, et al. (2010) Extension of lean and diluted combustion stability limits by using repetitive pulse discharges. *SAE Technical Papers* 1-12.
18. Pertl FA, Smith JE (2009) Electromagnetic design of a novel microwave internal combustion engine ignition source, the quarter wave coaxial cavity igniter. *Proceedings of the Institution of Mechanical Engineers Part D: Journal of Automobile Engineering* 223: 1405-1417.
19. Kettner M, Andreas N, Spicher U, Seidel J, Linkenheil K (2006) Microwave-based ignition principle for gasoline engines with direct injection and spray guided combustion system. *Research Ignition* 67: 29-31.
20. DeFilippo A, Saxena S, Rapp VH, Dibble RW, Chen JY, et al. (2011) Extending the lean stability limits of gasoline using a microwave-assisted spark plug. *SAE Technical Paper* 1-12.
21. Rapp VH, DeFilippo A, Saxena S, Chen JY, Dibble RW, et al. (2012) Extending lean operating limit and reducing emissions of methane spark-ignited engines using a microwave-assisted spark plug. *Journal of Combustion* 2012: 1-8.
22. Ombrello T, Won SH, Ju Y, Williams S (2010) Flame propagation enhancement by plasma excitation of oxygen. Part I: Effects of O₃. *Combustion and Flame* 157: 1906-1915.
23. Ombrello T, Won SH, Ju Y, Williams S (2010) Flame propagation enhancement by plasma excitation of oxygen. Part II: Effects of O₂(a1Dg). *Combustion and Flame* 157: 1916-1928.
24. Sun W, Won SH, Ombrello T, Carter C, Ju Y (2013) Direct ignition and S-curve transition by in situ nano-second pulsed discharge in methane/oxygen/helium counterflow flame. *Proceedings of the Combustion Institute* 34: 847-855.
25. Groff EG, Krage MK (1984) Microwave effects on premixed flames. *Combustion and Flame* 56: 293-306.
26. Clements RM, Smith RD, Smy PR (1981) Enhancement of flame speed by intense microwave radiation. *Combustion Science and Technology* 26: 77-81.
27. Michael JB, Dogariu A, Shneider MN, Miles RB (2010) Subcritical microwave coupling to femtosecond and picosecond laser ionization for localized, multipoint ignition of methane/air mixtures. *Journal of Applied Physics* 108.
28. Wolk B, DeFilippo A, Chen JY, Dibble R, Nishiyama A, et al. (2013) Enhancement of flame development by microwave-assisted spark ignition in constant volume combustion chamber. *Combustion and Flame* 160: 1225-1234.
29. Sasaki K, Shinohara K (2012) Transition from equilibrium to nonequilibrium combustion of premixed burner flame by microwave irradiation. *Phys D: Appl Phys* 45.
30. Martinez-Frias J, Aceves SM, Flowers DL (2007) Improving ethanol live cycle efficiency by direct utilization of wet ethanol in HCCI engines. *J Energy Resour Technol* 129: 332-337.
31. Mack JH, Aceves SM, Dibble RW (2009) Demonstrating direct use of wet ethanol in a homogeneous charge compression ignition (HCCI) engine. *Energy* 34: 782-787.
32. Cummings J (2011) Effects of Fuel Ethanol Quality on Vehicle System Components. *SAE Technical Papers* 1-12.
33. Ikeda Y, Nishiyama A, Kaneko M (2009) Microwave enhanced ignition process for fuel mixture at elevated pressure of 1MPa. 47th AIAA Aerospace Sciences Meeting Including the New Horizons Forum and Aerospace Exposition, Orlando, Florida, US.
34. Fridman A, Kennedy L (2011) *Plasma Physics and Engineering*. (2nd edn), Taylor and Francis, Boca Raton, US.
35. Heywood JB (1988) *Internal Combustion Engine Fundamentals*. McGraw-Hill, New York.
36. Goodwin DG (2003) An open-source, extensible software suite for CVD process simulation." *Chemical Vapor Deposition XVI and EUROCVI 14*, ECS Proceedings, M Allendorf, F Maury, and F Teyssandier, editors, The Electrochemical Society 8: 155-162.
37. Woschni G (1967) A Universally Applicable Equation for the Instantaneous Heat Transfer Coefficient in the Internal Combustion Engine. *SAE Technical Papers* 1-19.
38. Lavoie GA, Martz J, Wooldridge M, Assanis D (2010) A multi-mode combustion diagram for spark assisted compression ignition. *Combustion and Flame* 157: 1106-1110.
39. Lelevkin VM, Otorbaev DK, Schram DC (1992) *Physics of Non-Equilibrium Plasmas*. Elsevier Science Publishers, Amsterdam.
40. Bayraktar H (2005) Experimental and theoretical investigation of using gasoline-ethanol blends in spark-ignition engines. *Renewable Energy* 30: 1733-1747.